

Removal of Phenol from Water Using ZnO Nanoparticles

Abdulkareem Hammoodi Assaf¹, Asmiet Ramizy*², Ahmed Mishaal Mohammed³

¹ Center of Desert Studies - University of Anbar

²Department of Physics -College of Science – University of Anbar

³Department of Chemistry - College of Science- University of Anbar

*Corresponding author²: asmad_hadithi@uoanbar.edu.iq

Abstract

Zinc oxide (ZnO) nanoparticles were prepared using a pulsed laser ablation (PLA) method with various laser energies of 100, 200, 300, 400 and 500 mJ for removing organic pollutants, (phenol), from water solutions. The acquisition of ZnO nanoparticles with nanoparticle size was confirmed using XRD tests. Zeta Potential (Z.P.) tests showed that the prepared nanoparticles were electrically unstable. The prepared particles were used to remove the dissolved solvent (phenol) in the water resulting from many industries. Results showed that the obtained removal percentage of organic pollutants (phenols) ranged from 90% to 93.86%.

Keywords: PLA, ZnO, Phenol, Pollutant removal, Nanoparticles, Adsorption.

1. Introduction

As one of the most important sources of life in our planet, water could be considered a primary resource. No life exists without water, and where water is found, life [1], civilisations, villages, and cities also prosper. Thus, must preserve the wealth is one of the most important corners of life .Rivers and seas are the main water source which are the essential requirement for world population. However, numerous pollutants are released into rivers and seas, regardless of whether they are organic, inorganic or radioactive. Thus, water sources should be free from these pollutants or at least contain pollutants within the permissible and non-harmful limits to the environment or its essential elements [2].

The most prominent organic pollutants include phenols and their compounds, which are produced from dyes, oil residues, hospitals and tanneries [3,4]. Owing to erroneous behaviour and neglect, such as dumping of pollutants, rivers are unsuitable for natural and human use. Phenols can be classified as one of the most dangerous organic compound contaminants in water, a small percentage of which show toxicity [5]. Phenol endangers human health mainly as it causes a number of serious diseases, including hepatitis and kidney failure. High phenol levels may lead to other diseases, such as diarrhoea, dark urine, destruction of red blood cells and possibly cancer; the maximum limits of phenol should be $20 \mu\text{g} \cdot \text{l}^{-1}$, and studies should search for solutions to eliminate this contaminant [4,6].

Various methods, such as elimination of contaminants (phenols) by charcoal derived from coconut husk, are used to treat pollution caused by chemical processes. The best results include the removal of 49.7%–67.9% of phenols and compounds [7]. However, the temperature must be effective and efficient. The domestic markets feature low quantities and expensive prices of coconut [7]. Recently, ZnO Particle size up to 140 nm prepared by sol-gel method and the best time to remove the phenol was 120 minutes with rate of 82%. The initial concentration of pollutants was only 55 ppm [8]. Other methods have emerged to exploit the properties of nanoparticles as they possess different characteristics compared with original materials of life Nanoparticles act as membranes to prevent water leakage, and they contain bacteria and viruses [4].

In this study, ZnO, which is locally available in large amounts, will be treated as a liquid phase to prepare its nanoparticles in simple technique with no negative side effects using pulse laser ablation (PLA) to remove of phenol pollution from water.

2. Materials and methods

2.1. Preparation of liquid-phase nanoparticles (liquid medium):

Bulk ZnO was used to prepare pellets with diameter of 2 cm, and 6 mm height under a pressure of 400 bar for period of 24 h. the sample placed in an oven at temperature of 600°C for 4 h and then left to cool for up to 24 h. The above pellets were then immersed in 15 ml double-distilled water. ZnO nanoparticles perpetration conditions: as shown in the table (1)

Table (1):ZnO nanoparticles perpetration conditions

| No. | Materials | Pellets properties | | | | |
|-----|-------------------|--------------------|-----------|----------|---------------------------|--------|
| | | Diameters | Height | Pressure | Time | Temp. |
| 1 | ZnO | 2 cm | 6 mm | 400 bar | 4 h | 400 °C |
| 2 | ZnO nanoparticles | Conditions | | | | |
| | | Wavelength | Frequency | Pules | Energy | |
| | | 1064 nm | 6 Hz | 300 | 100,200, 300, 400 and 500 | |

2.2 Preparation of 100ppm pollutant phenol solution

Standard solution was prepared with a concentration of 1000 ppm phenol with 99%purity in a 1000 ml bottle. Then, ion-free water (500 ml) was added, and the solution was stirred well until material dissolution for 15 min. The desired volume was completed with double-distilled water similar to the above solution.

2.3 Determination of wavelength location and calibration curve

Wavelength was determined at the highest absorption of phenol–water solution by absorbance spectrometry using a UV-visible spectrometer (T80 UV/Vis spectrometer, PG Instruments Ltd) within the range of 200-400 nm. Observations showed a substance absorption peak at 270 nm wavelength of phenol in the standard curve [9] as found in shown Figure (1).

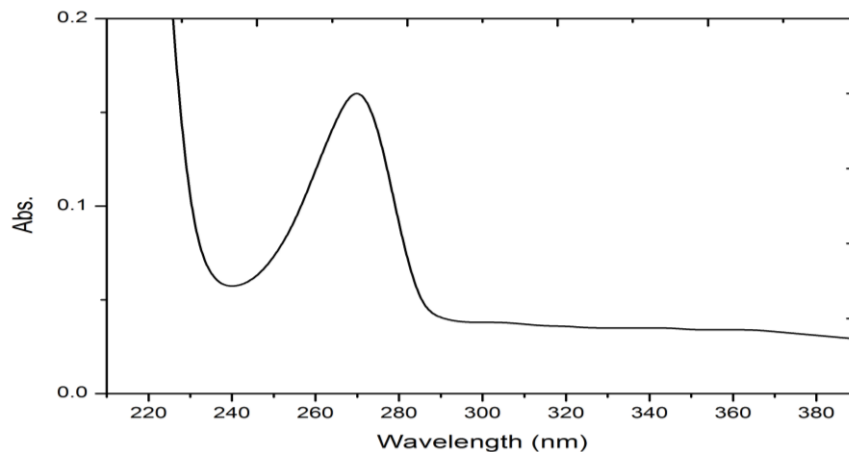


Figure (1): Spectral absorption (UV-Vis) of phenols

To determine the calibration curve for the standard solutions, phenol solutions were prepared at different concentrations (1, 2, 3, 4, 5, 6, 7, 8, 9 and 10 ppm). Then, the phenol value (λ_{\max}) and absorbance indicating the solubility of solutions were fixed by calibration based on Beer-Lambert's law, which represents the relationship between absorbance and concentration [10] Figure (2).

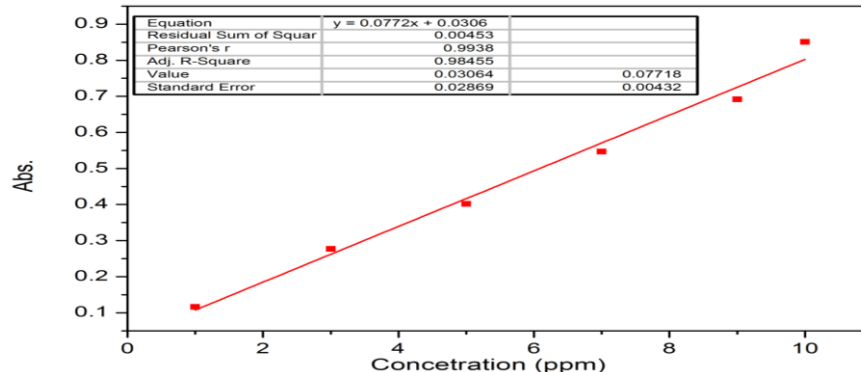


Figure (2): Standard calibration curve for standard phenol solutions prepared at 270 nm wavelength at varying concentrations

2.4 Measurements of the prepared particles

The resulting material was subjected to laser treatment with the lowest and highest laser energies of 100 and 500 mJ, respectively, at which nanoparticles were prepared. We employed X-ray diffraction (XRD) (D2 PHASER), to investigate the structure which recorded the intensity as a function of Bragg's angle of the material, crystalline nature, particle size and crystalline arrangement. XRD measurements were performed on the material and compared with diffraction data (standard) card No. (96-901-1663) [11].

SPMAA 3000 Angstrom Advanced was used for atomic force microscopy (AFM). This technique is used to determine the exact details on surface morphology to identify the shape of particles and ensure that nanoparticles have been achieved.

To identify electrical cells, zeta potential was tested, and Brookhaven Instruments (United States) was used to assess particles ranging from 1nm to 30 μm . Zeta potential is an important parameter as it is used to gain insights into biological systems, such as blood, function and pharmaceuticals. Zeta potential also plays an important role in dyeing, inks and clay turbidity, depending on the polarity of solution ions and surface area of the material.

A stable polarity is needed in zeta voltage applications, but in our research, we have benefited from the instability of electrical nanoparticles, which were designed to attract and capture pollutants.

2.5 Isotherm adsorption

Phenol adsorption was carried out in a water solution. To obtain adsorption from phenol-based solutions, 5 ml silty material containing nanoparticles from ZnO was added to each sample in 25 ml bottle, and each phenol solution (5 ml) with 100 ppm phenol was sealed tightly in volumetric bottles, mixed and then placed in a water bath with vibrating temperature of 25°C at different periods of continuous shaking (10–80) min. For each 10 min of recording the readings, the samples was removed every 10 min of continuous shaking. These samples were separated by centrifugation (4000 cycles.min⁻¹ for 10 min), while absorption of solutions was evaluated by UV spectrometer–visible spectrophotometer. The equilibrium concentration was adjusted from the calibration curve in Figure (2).

The amount of absorbent material was calculated in all cases under Equation (1) [10]:

$$\text{con.} = \frac{\text{Abs.} - \text{Intercept}}{\text{slope}} \quad \dots \dots \quad (1)$$

Where:

Con = Concentration of phenol; Abs = Absorption.

The percentage of absorption t concentration or pollutant concentration after treatment (pollutant-free purification) was calculated by Equation (2) [12]:

$$\text{R\%} = \left[\frac{(C_o - C_e)}{C_o} \right] \times 100 \quad \dots \dots \quad (2)$$

Where:

R% = percentage of adsorption (percentage of removal)

C_o = Primary concentration (ppm), C_e = Focus at equilibrium (ppm).

3. Results and Discussion

3.1 X-ray studies of structural properties

XRD showed that the nanoparticles as particles in a hexagonal structure, which are prepared in the liquid phase at the lowest and highest laser energies that were a pure ZnO material. This finding agrees with the results of previous studies [13,14]. Six different values corresponded to the 100,002,101,102,110 and 103 planes and angles of 31.693° , 34.344° , 36.184° , 47.457° , 56.188° , and 62.791° . The dominant trend was the 100 plane, as described in Figures (3) and (4) and Tables (2) and (3) for energies of 100mJ and 500mJ, respectively, and these results in agreement with (standard) card No. (96-901-1663)[11].

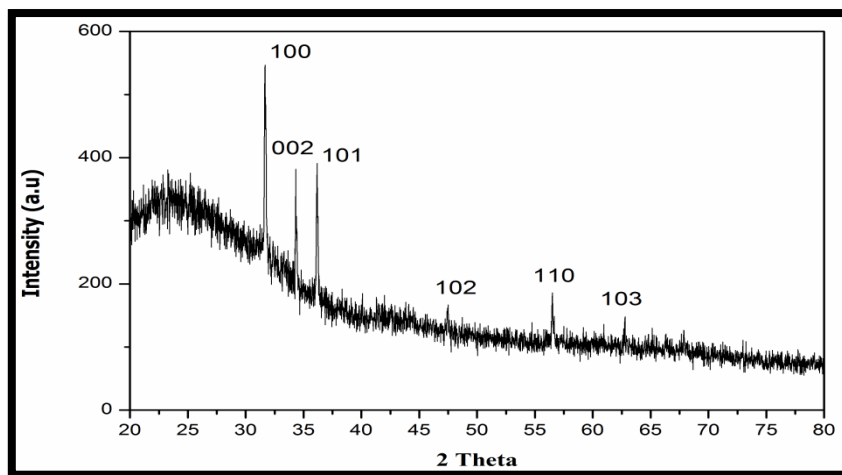


Figure (3): XRD patterns of ZnO nanoparticles at laser energy of 100 mJ

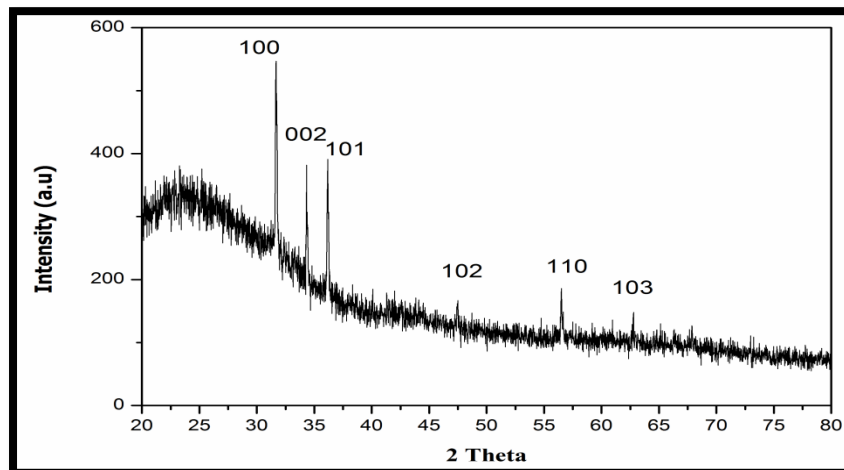


Figure (4): XRD patterns of ZnO nanoparticles at laser energy of 500mJ

Table (2): Values 2θ and FWHM of ZnO nanoparticles at laser energy of 100mJ

| 2θ (Deg.) | d (Å) | Area% | FWHM (Deg.) |
|------------------|--------|-------|-------------|
| 31.693 | 2.8209 | 100.0 | 0.172 |
| 34.344 | 2.6090 | 45.5 | 0.173 |
| 36.184 | 2.4804 | 58.5 | 0.189 |
| 47.457 | 1.9142 | 14.6 | 0.272 |
| 56.518 | 1.6269 | 19.4 | 0.242 |
| 62.791 | 1.4786 | 9.6 | 0.217 |

Table (3): Values 2θ , and FWHM of ZnO nanoparticles at laser energy of 500mJ

| 2θ (Deg.) | d (Å) | Area% | FWHM (Deg.) |
|------------------|--------|-------|-------------|
| 31.674 | 2.8225 | 100.0 | 0.205 |
| 34.344 | 2.6090 | 28.0 | 0.138 |
| 36.166 | 2.4816 | 61.0 | 0.189 |
| 47.526 | 1.9116 | 18.9 | 0.556 |
| 56.499 | 1.6274 | 25.8 | 0.233 |
| 62.753 | 1.4794 | 17.6 | 0.283 |

The crystal size value was calculated using Scherer formula (3) [15].

$$G = \frac{0.9\lambda}{\Delta(2\theta)\cos\theta_B} \quad \dots \dots \quad (3)$$

where:

2θ = full width at half maximum (FWHM) by radian and at the extreme mean

λ = falling X-ray wavelength; θ_B = brack angle.

0.94 = Scherer's constant.

The nanoparticle crystal sizes were obtained as shown in Table (4). The findings are consistent with the results in [16].

Table (4): Size of nanoparticles prepared at 100 mJ and 500 mJ laser energies

| Energy (mJ) | 2Theta ($2\theta^\circ$) | FWHM | Crystal size (nm) |
|-------------|----------------------------|-------|-------------------|
| 100 | 31.693 | 0.172 | 50.17 |
| | 34.344 | 0.173 | 50.22 |
| | 36.184 | 0.189 | 46.20 |
| 500 | 31.674 | 0.205 | 42.09 |
| | 34.344 | 0.138 | 62.96 |

| | | | |
|--|--------|-------|-------|
| | 36.166 | 0.189 | 45.97 |
|--|--------|-------|-------|

3.2. Study of morphological characteristics (AFM)

Morphological characteristics at the lowest and highest energies were examined using AFM Figs. 5 and 6 show the two- and three-dimensional images of the particles prepared at the lowest and highest energies, respectively. The average nanoparticle diameter was 73.84 nm, and the liquid in the laser used 100 mJ of energy in the PLA system. When the estimated energy was 500 mJ, the resulting particle size was 92.80 nm, as indicated in Table (5) and (6). The size of heated nanoparticles increased after the elimination process due to high temperature [17]; the average root mean square (RMS) also increased, indicating the increasing rate of roughness with increasing laser energies, corresponding to previously reported findings [18].

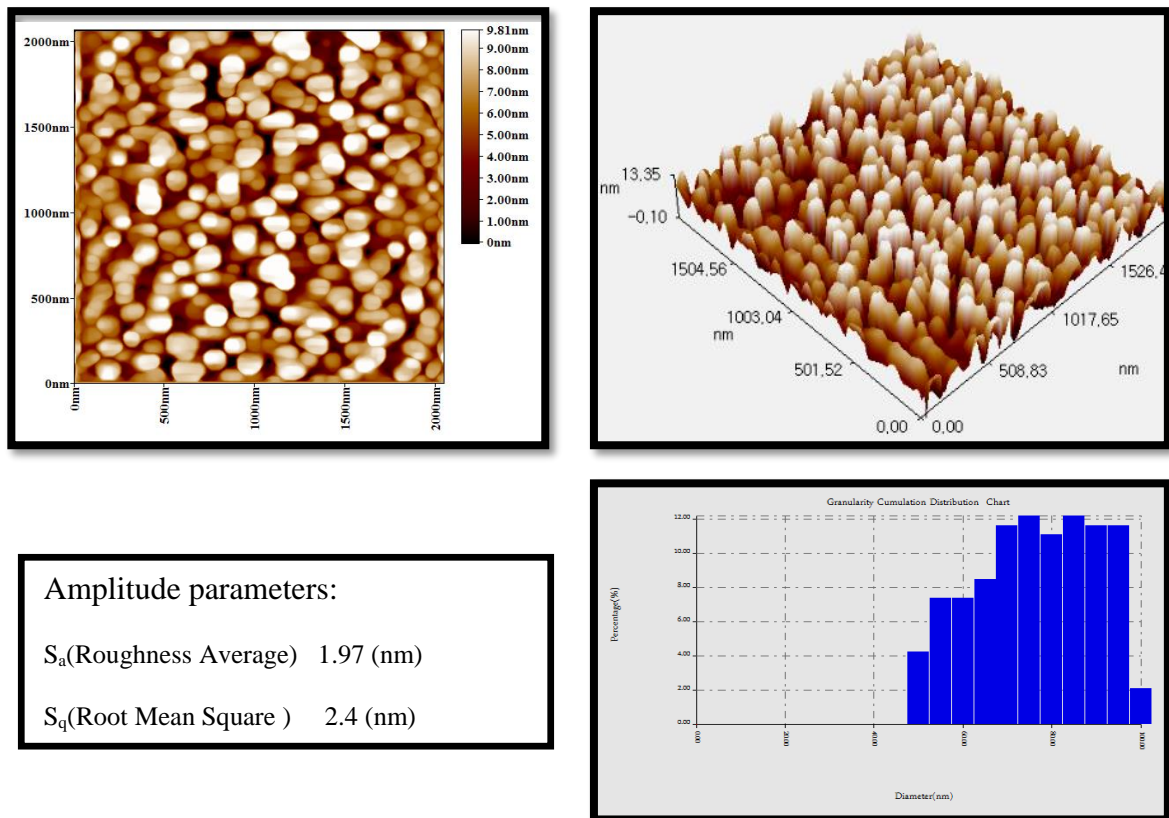
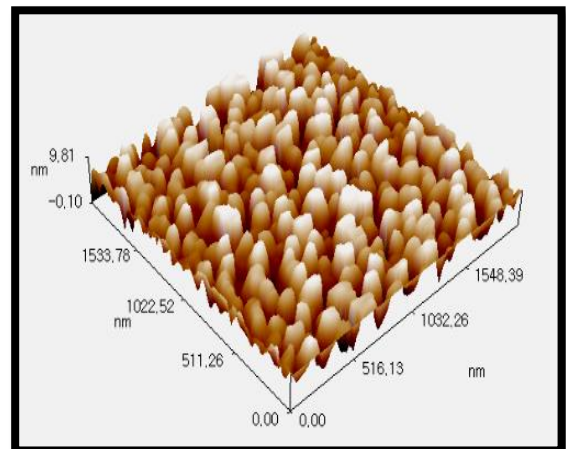
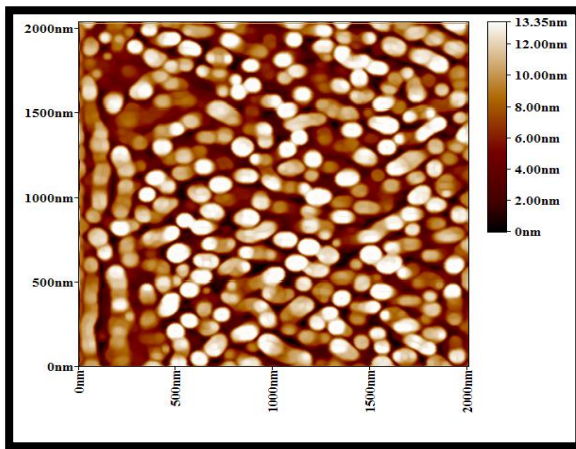


Figure (5): Two and three -dimensional images of nanoparticles prepared at 100mJ energy and 74.84 nm wavelengths.

Table (5): size of nanoparticles prepared at 100 mJ laser energy

| Diameter(nm)< | Volume(%) | Cumulation(%) | Diameter(nm)< | Volume(%) | Cumulation(%) | Diameter(nm)< | Volume(%) | Cumulation(%) |
|---------------|-----------|---------------|---------------|-----------|---------------|---------------|-----------|---------------|
|---------------|-----------|---------------|---------------|-----------|---------------|---------------|-----------|---------------|

| | | | | | | | | |
|-------|------|-------|-------|-------|-------|--------|-------|--------|
| 50.00 | 4.23 | 4.23 | 70.00 | 11.64 | 39.15 | 90.00 | 11.64 | 86.24 |
| 55.00 | 7.41 | 11.64 | 75.00 | 12.17 | 51.32 | 95.00 | 11.64 | 97.88 |
| 60.00 | 7.41 | 19.05 | 80.00 | 11.11 | 62.43 | 100.00 | 2.12 | 100.00 |
| 65.00 | 8.47 | 27.51 | 85.00 | 12.17 | 74.60 | | | |



Amplitude parameters:
 S_a (Roughness Average) 3.1 (nm)
 S_q (Root Mean Square) 3.63

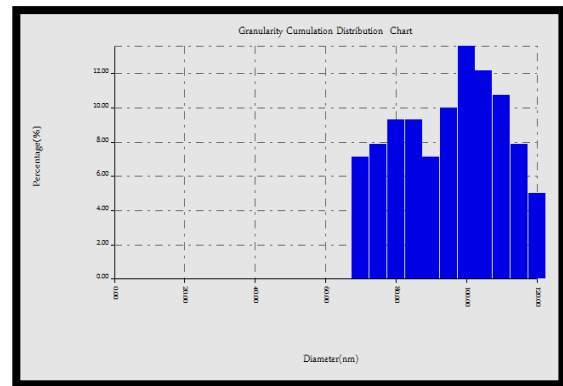


Figure (6): Two and three-dimensional images of nanoparticles prepared at 500 mJ energy and 92.80 nm wavelength

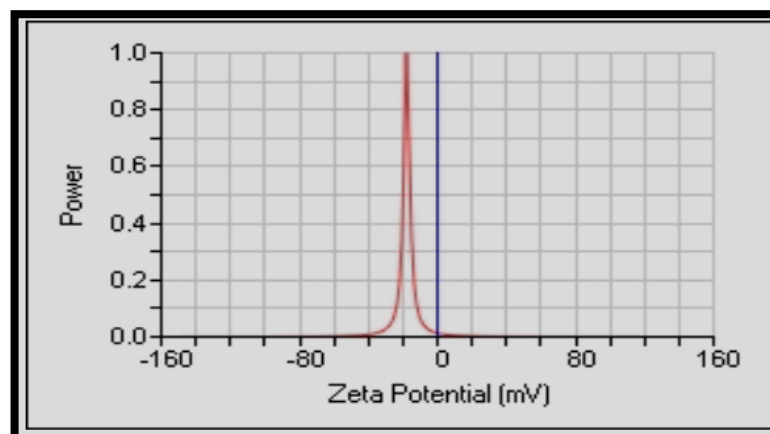
Table (6): Size of nanoparticles prepared at 500mJ laser energy

| Diameter(nm)< | Volume(%) | Cumulation(%) | Diameter(nm)< | Volume(%) | Cumulation(%) | Diameter(nm)< | Volume(%) | Cumulation(%) |
|---------------|-----------|---------------|---------------|-----------|---------------|---------------|-----------|---------------|
|---------------|-----------|---------------|---------------|-----------|---------------|---------------|-----------|---------------|

| | | | | | | | | |
|-------|------|-------|--------|-------|-------|--------|-------|--------|
| 70.00 | 7.14 | 7.14 | 90.00 | 7.14 | 40.71 | 110.00 | 10.71 | 87.14 |
| 75.00 | 7.86 | 15.00 | 95.00 | 10.00 | 50.71 | 115.00 | 7.86 | 95.00 |
| 80.00 | 9.29 | 24.29 | 100.00 | 13.57 | 64.29 | 120.00 | 5.00 | 100.00 |
| 85.00 | 9.29 | 33.57 | 105.00 | 12.14 | 76.43 | | | |

3.3. Electric cell study

Zeta potential was determined for ZnO nanoparticles prepared at 100 mJ which was -17.75mV as shown in figure (7). At 500 mJ, the voltage was -20.3mV, as shown in Fig. (8). This finding indicates that the nanoparticles are electrically unstable; as shown in Table (7), the nanoparticles generally searched for different polarity ions to combine with melted soluble phenols, corresponding to the result in [19]. By separating the centrifuged material, the contaminant, which has enlarged due to assembly, was disposed with electrolytic and non-stable preparation of particles.



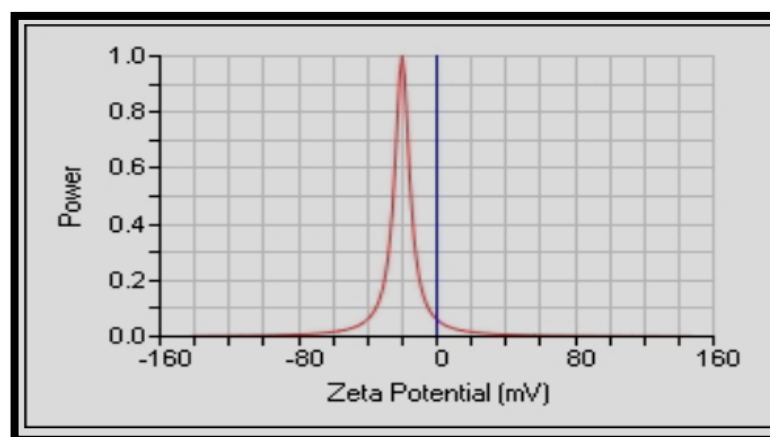
Results

Zeta potential (mv) : -17.75

Analysis Type : Smoluchowski

Mobility (μ /s)/(v/cm) : -1.39

Figure (7): Zeta potential of ZnO nanoparticles prepared at laser energy of 100 mJ

**Results**

Zeta potential (mv) : -20.03

Analysis Type : Smoluchowski

Mobility (μ/s)/(v/cm) : -1.57

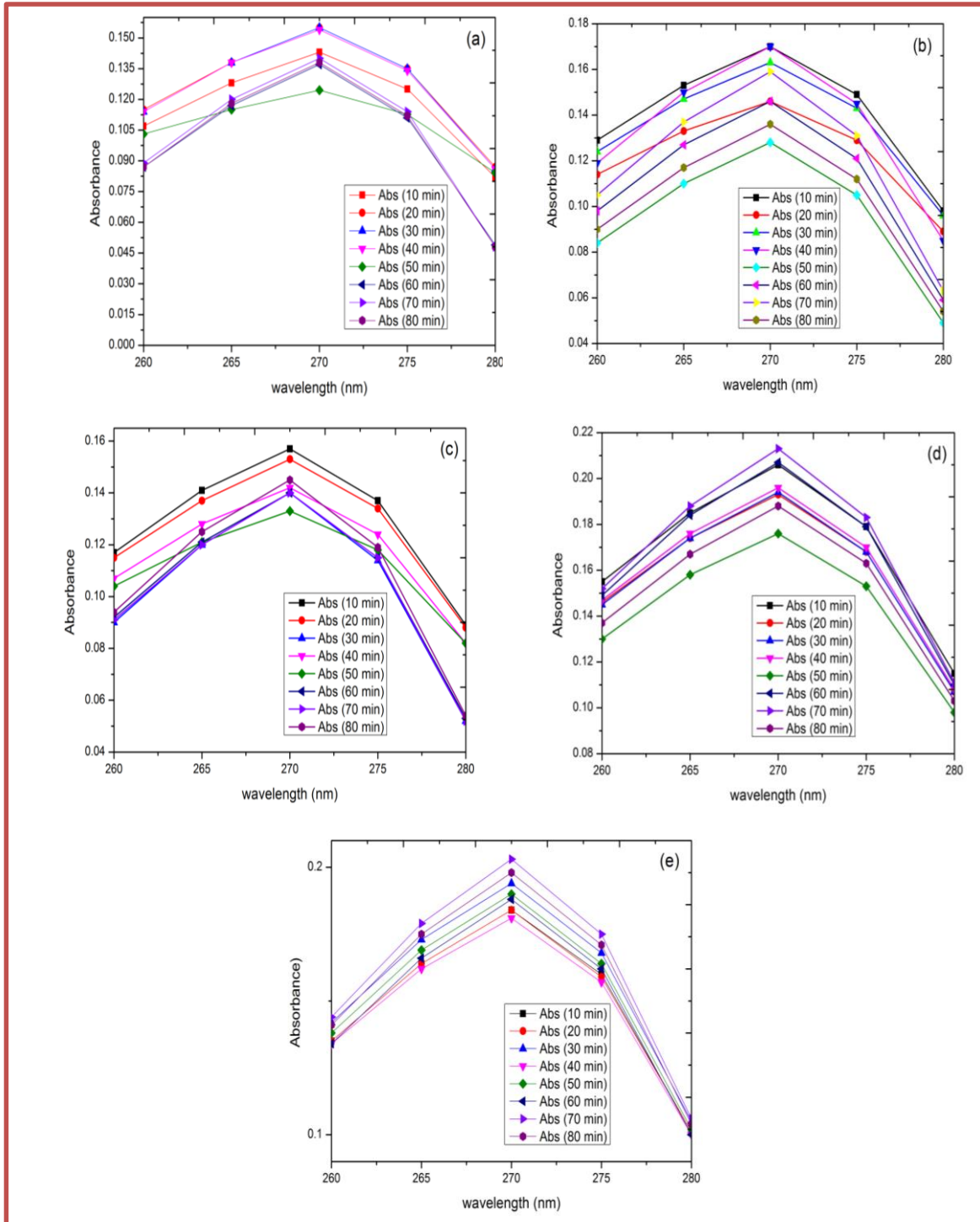
Figure (8): Zeta potential of ZnO nanoparticles prepared at laser energy of 500 mJ

Table (7): Electrical stability ranges of nanoparticles [20]

| Zeta Potential (mV) | Stability behavior of the colloid |
|---------------------------|-----------------------------------|
| from 0 to ± 5 | Rapid coagulation or flocculation |
| from ± 10 to ± 30 | Incipient instability |
| from ± 30 to ± 40 | Moderate stability |
| from ± 40 to ± 60 | Good stability |
| more than ± 61 | Excellent stability |

4.3 Measurement of pollutant concentration after treatment

Absorption was calculated by UV-visible spectrometry at the energies used in preparation of nanoparticles and at 300 pulse.min⁻¹ pulses within the range of 260-280 nm every 10 min and at the contact time of 10-80 min during removal of ZnO nanoparticles in phenol Figure(9).



mJ

10) at
own in

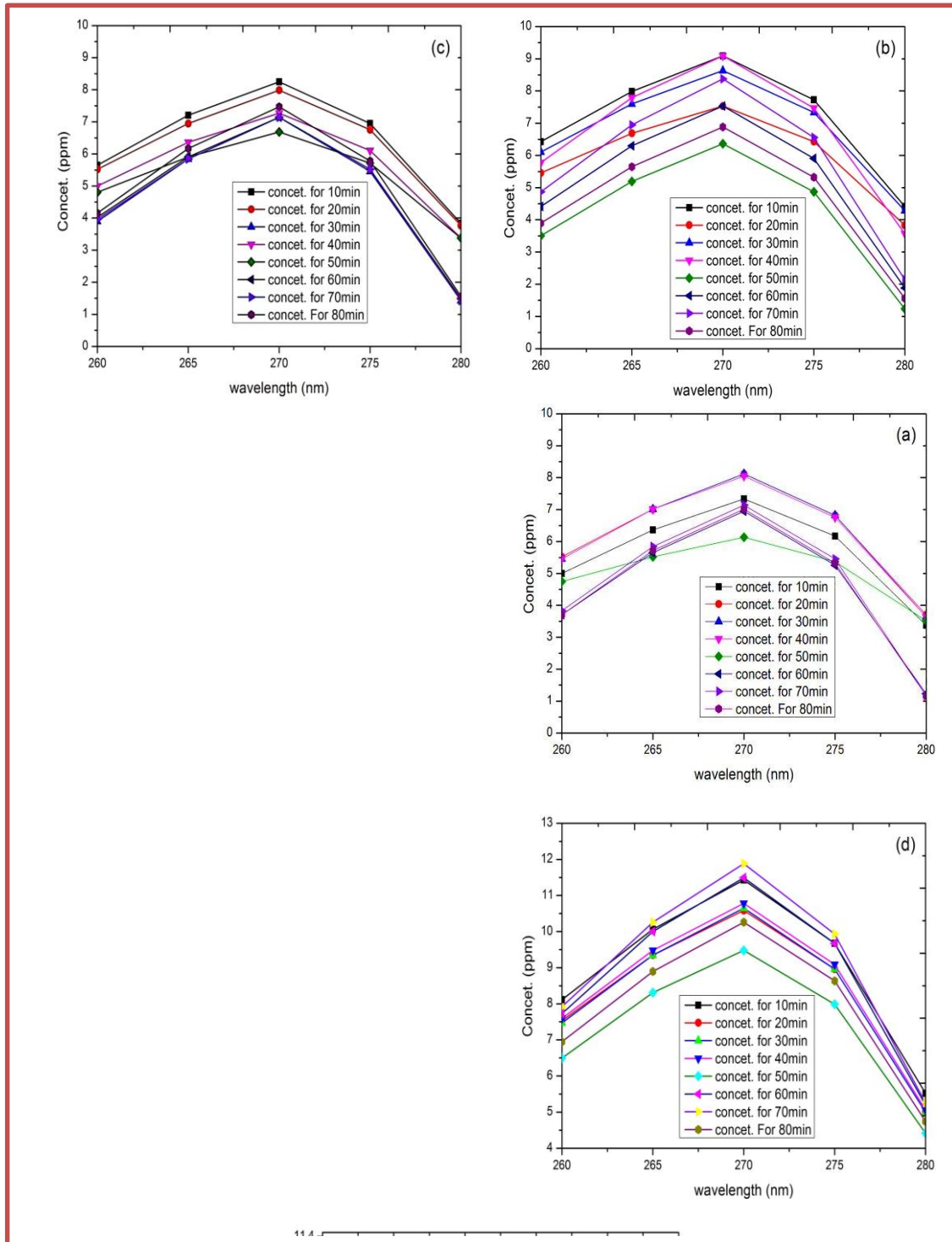


Figure (10): Concentration of nanoparticles prepared at: (a) 100mJ, (b) 200mJ,(c) 300mJ, (d)400mJ ,(e)500mJ

The best results for phenol removal after treatment with ZnO nanoparticles were noted at $\lambda_{\max} = 270$ nm at 25°C [9]. The lowest concentration after treatment was 6.136 ppm according to Equation (2). The percentage of adsorption after treatment reached 93.864% according to Equation (3). As shown in Table (8) the smallest granular size of the nanoparticles prepared were used according to the parameters mentioned above at 100 mJ. This finding is due to the increased concentration of nanoparticles prepared in accordance with the parameters mentioned above, featuring a higher surface area and a relatively larger surface compared to possessing a small particle size. Notably, the percentage of phenol removal at the first 10 min is about 89%–90% as a result of the large surface area of adsorption. This finding is consistent with the of adsorption kinetic as initial adsorption occurred rapidly and then slowed down due to the work on most of the surface area of the adsorbent substance, consistent with the findings in [21].

(8):
of

| Percentage of removal (R %) | Concentration (ppm) | Best adsorption time (min) | Energy(mJ) |
|-----------------------------|---------------------|----------------------------|-------------|
| 93.864 | 6.136 | 50 | 100 |
| 93.637 | 6.363 | 50 | 200 |
| 93.312 | 6.688 | 50 | 300 |
| 90.519 | 9.481 | 50 | 400 |
| 90.195 | 9.805 | 40 | 500 |

Table
Rates
phenol

adsorption from water solution at a primary concentration of 100ppm

4. Conclusions:

ZnO nanoparticles were obtained as hexagonal composition phase according XRD measurements and the images which show small size nanoparticles after the pulsed laser treatment, AFM result showed that the average root mean square (RMS) and the roughness was increased with increasing laser energies. Liquid-phase ZnO nanoparticles were obtained at 100 mJ of laser energy to eliminate the phenol contaminated user using ZnO nanoparticles Considering the time factor and importance of certain limits, the results showed

that the best period time to eliminate the phenol contaminated was (40-60) min at a rate of 93.86%.

References

1. Grigg, Neil S. "The business of water in a changing world: organizations, connectors and support sector." *International Journal of Water Resources Development*, Vol.32,708-720, (2016).
2. Elijah Ramsey III, Ira Leifer, Bill Lehr, Xiaofeng Li and Prasad S. Thenkabail," Satellite Survey of Inner Seas: Oil Pollution in the Black and Caspian Seas", *Remote sens*, 8(10), 875, (2016).
3. Villegas, Laura G. Cordova, et al. "A short review of techniques for phenol removal from wastewater." *Current Pollution Reports* Vol. 2, 157-167, (2016).
4. Alexander, M. ,"Microbial technologies to overcome environmental problems of persistent pollutants", Publication of the United Nations Environment Programme, Nairobi, 5-15, (1987).
5. Hassan, H. Shokry, et al. "Synthesis and Characterization of Zinc Oxide Nanoparticles Using Green and Chemical Synthesis Techniques for Phenol Decontamination." *International Journal of Nanoelectronics and Materials*, Vol, 11.2 179-193, (2018).
6. . Al-Hashimi, Amna MA. "Biodegradation Effect of some Bacterial Isolates on some Endocrine Disruptors (EDCS)." *Al-Mustansiriyah Journal of Science* Vol.29, 43-49, (2018).
7. Lekaa, H. K. ,and Abbas, H. Al-Khafaji," Thermodynamic Study of phenol ,O-hydroxy phenol ,p-amino phenol and 2,4,6-trinitro phenol Adsorption charcoal derived from coconut shell", *journal of kerbala university*, Vol.: 8 (1), 307-315, (2010).
8. Yusoff, Nikathirah, et al. "Enhanced photodegradation of phenol by ZnO nanoparticles synthesized through sol-gel method." *Sains Malaysiana* Vol.46 , 2507-2514, (2017).
9. Sharma, Y. R. "Elementary organic spectroscopy, principles and chemical application." Chand and Company Ltd, New Delhi, India, 23, (2009).
10. Alkines, P. W. , " *Physical Chemistry* ", 4th ed., Oxford University press, (1996).
11. Xu, Y. N.,and Ching W. Y., "Electronic, optical, and structural properties of some wurtzite crystals", *Physical Review B* 48, 4335-4351, (1993).
12. Lekaa, H. A.,and Al-Sammrae, J.," Study of The Factors Affecting The Adsorption of Some Azo Dyes By Using Different Adsorbents", A Thesis Submitted, of the College of Education for Women University of Tikrit, (2006).
13. Khorsand, Z., Razali, R., Abd Majid, WH., and Majid D.," Synthesis and characterization of a narrow size distribution of zinc oxide nanoparticles", *International Journal of Nanomedicine*,vol.6, 1399-1403, (2011).
14. Erhaima, M. K., " Structural and Optical Properties of ZnO:Co (CZO) Thin Films Prepared by Chemical Spray Pyrolysis Method", M.Sc.Thesis, University of Baghdad ,(2010).
15. Hammed, Q. K. "Thin film Carbon nanotube/polymer polymerized by plasma as humidity sensor", Thesis Submitted to the council of the College of science University of Anbar, (2017).
16. Guillén, G. García, et al. "Structure and morphologies of ZnO nanoparticles synthesized by pulsed laser ablation in liquid: Effects of temperature and energy fluence." *Materials Chemistry and Physics* ,Vol.162 , 561-570, (2015).
17. Taus J., "Amorphous and Liquid Semiconductors", Plenum Press, London, (1974).
18. Fattin, A. F.,and Iman, H. H.," Preparation and characterization of zinc oxide nanoparticles by laser ablation of zinc in isopropanol", *Eng.&Tech. Journal*,Vol.33, part(B), No.5, (2015).

19. Marsalek, Roman. "Particle size and zeta potential of ZnO." APCBEE procedia 9 , New Delhi, India, 13-17, (2014).
20. Hunter, Robert J. Zeta potential in colloid science: principles and applications.Vol.2 , Academic press, (2013).
21. Aslam, M. M. , I. Hassan , M. Malik and A. Matin, " Removal of Copper from Industrial Effluent by Adsorption with Economical Viable Material Institute of Environmental Sciences and Engineering National University of Sciences and Technology Pakistan, 2005.